URBAN WATER JOURNAL
2023, VOL. 20, NO. 9, 1219–1230
https://doi.org/10.1080/1573062X.2023.2254739

Taylor & Francis
Taylor & Francis Group

RESEARCH ARTICLE

Deciphering and predict corrosion effect, influencing factors and microbial mechanism of sewer concrete corrosion based on extensive data analysis and machine learning

Wenhao Wang[a], Xinxin Xu[b], Jingguo Cao[a], Ming Zeng[c] and Wu Zhang[c]

[a]College of Chemical Engineering and Material Science, Tianjin University of Science & Technology, Tianjin, China; [b]Department of Environmental Engineering, College of Environmental & Resource Sciences, Zhejiang University, Hangzhou, China; [c]College of Marine and Environmental Sciences, Tianjin University of Science & Technology, Tianjin, China

ABSTRACT

This study investigated the effect of environmental parameters on microbial-induced concrete corrosion during three corrosion stages. The corrosion effects and influencing factors in three corrosion stages were deeply analyzed and predicted, and the mechanism of microbial corrosion was summarized. When the H_2S concentration was lower than about 15.0 mg/m^3, the corrosion was maintained in stage II, which greatly delays the intensification of corrosion. In stage III, the H_2S concentration has the significantly accelerate the corrosion rate. Additionally, incorporating min, max and mean values of input parameters greatly improved the accuracy of machine learning predictions of corrosion rates (R^2 >0.99). *Acidithiobacillus* was found to be dominant in the microbial community at H_2S concentrations of 12.0–37.5 mg/m^3, and increased temperature promoted the reproduction of *Acidithiobacillus*.

ARTICLE HISTORY
Received 19 April 2023
Accepted 24 August 2023

KEYWORDS
Sewer corrosion; concrete; environmental parameters; machine learning; microbial community

1. Introduction

Concrete degradation due to microbially induced concrete corrosion (MICC) has been a basic problem inside the international's underground infrastructure for the final century (Jiang et al. 2015; Grengg et al. 2017). For example, the annual cost of basic measures to repair wastewater is enormous. In the United States, the United Kingdom, Germany and Australia, the total length of sewer installations continues to expand as populations increase and cities expand (Abuhishmeh and Jalali 2023). In recent studies, radar monitoring of corrosion depth has also been widely used in drainage pipes but this is undoubtedly expensive (Ebrahimi and Jalali 2022a, 2022b). Crucial repairs to sewer infrastructure are pricey each year, and protection costs boom as sewers age (Grengg et al. 2018; Jiang et al. 2015; O'connell, Mcnally, and Richardson 2010).

MICC in the sewer is mainly concentrated in the ceiling of the sewer (crown area) and the wall position above the sewage (tidal area) (Cayford et al. 2012; Li 2020; Song et al. 2019). Gaseous hydrogen sulfide, carbon dioxide, methane, and other volatile organic compounds (VOCs) are degassed into the sewer pipe. Concrete corrosion caused by microorganisms is usually affected by environmental factors, mainly gas-phase H_2S concentration, temperature (temp.), and relative humidity (RH) (Joseph et al. 2012; Okabe et al. 2007; Sun et al. 2014; Vollertsen et al. 2008). Concrete corrosion is a complex process attacked by chemically and biologically generated organic and inorganic acids (Wang et al. 2022). Although concrete sewer corrosion is mostly a microbial process, it can become a chemical process at very high H_2S concentrations (Li et al. 2019).

The degradation of concrete caused by MICC can be summarized into three stages according to the surface pH. In stage I, the surface pH is about 9–12, gaseous hydrogen sulfide, carbon dioxide, methane, and other volatile organic compounds VOCs diffuse and accumulates on the surface of the pipe wall to reduce the surface pH (Yuan et al. 2015). Because the initial concrete surface pH is too high, it is not conducive to the survival of sulfur-oxidizing bacteria (Allahverdi and Škvára 2000; Gutberlet, Hilbig, and Beddoe 2015; Ismail et al. 1993; Joseph et al. 2012).In stage II, when the pH of the concrete surface pH dropped to around 9, neutral sulfur oxidizing microorganism colonies first formed on the concrete surface (Bielefeldt et al. 2010). In stage III, when the surface pH was around 4, acidophilic sulfur-oxidizing microorganisms gradually replaced neutral sulfur oxidizing microorganism with increasing acidity and continued to oxidize sulfide to sulfuric acid. Analysis of surface microbial ecological structure benefits understanding and mitigating sewer corrosion (Li et al. 2017). *Acidiphiliums*, *Acidithiobacillus*, *Mycobacterium* have been shown to appear in MICC in previous articles. *Acidithiobacillus*, *Mycobacterium* has been found on severely corroded concrete surfaces under low pH conditions and is present in the final stages of corrosion.

Although there are many previous studies on MICC, there needs to be more comprehensive field and laboratory data to analyze the MICC process. In order to better simulate field data, the microbial corrosion acceleration chamber would also fluctuate environmental variables (Sun et al. 2015, 2019). Moreover, the prediction accuracy of field data needs to be improved. Corrosion rate, surface pH, and microbial community under

CONTACT Jingguo Cao cjg@tust.edu.cn; Ming Zeng ming.zeng@tust.edu.cn
Supplemental data for this article can be accessed https://doi.org/10.1080/1573062X.2023.2254739

different environmental factors are extracted from the literature for comprehensive analysis and prediction. Low surface pH is due to corrosion, usually calcium silicate hydrate (C-S-H), reacting to form sulfates such as gypsum. The reaction between gypsum and alumina produces ettringite, which will lead to the instability of the internal structure of the concrete and the formation of cracks, which will lead to a decrease in the strength of the concrete. Microorganisms colonize the concrete surface to continuously produce acid to cause acid penetration, which reduces the surface pH and further causes more serious corrosion, and then judges the corrosion situation. In recent years, machine learning regression algorithms have been widely used in environmental prediction and have shown good prediction performance (Ebrahimi, Hojat Jalali, and Sabatino 2023; Jiang et al. 2023; Wang et al. 2022). The machine learning algorithm has an excellent ability to predict nonlinear and complex regression (Abuhishmeh 2019). It has been proved to have a good prediction effect in predicting the corrosion initiation time and rate (Jiang et al. 2016; Li et al. 2019; Liu et al. 2017; Wang et al. 2022). Previous studies considered temperature, RH, H_2S concentration, and concrete location in sewers as critical environmental parameters, and a large number of laboratory and field datasets were generated in subsequent studies (Jiang, Keller, and Bond 2014; Satoh et al. 2009). However, because the previous forecasts with large fluctuations in field data could have been better (Deng et al. 2021; Jiang et al. 2016; Liu et al. 2017; Zounemat-Kermani et al. 2020), this paper added the maximum, minimum and average values of the fluctuation data to make predictions. Surface pH can easily obtain data and can well reflect the corrosion stage (Joseph et al. 2012; Satoh et al. 2009), so corrosion stage is added to verify whether the prediction accuracy of machine learning can be improved (Wang et al. 2023).

To sum up, this research mainly collects data to explore (1) the influence of environmental factors on the corrosion of sewer concrete under different stages, (2) adding the maximum, minimum and average values to improve the surface pH and corrosion rate of different machine learning models in terms of predictive performance, (3) the mechanism of microbial corrosion, the influence of stage III environmental factors and surface pH on the succession of microbial communities.

2. Materials and methods

2.1. Datasets collection

The surface pH database was established as shown in Table A.1, 833 surface pH data points (Jiang et al. 2015; Jiang, Keller, and Bond 2014; Lu 2019; Wells and Melchers 2014) were collected in three stages of MICC using ORIGIN software (2019b). Due to the fluctuation of field data and microbial corrosion acceleration chamber conditions, in order to better predict the surface pH, the maximum, minimum and average values of H_2S concentration temperature and RH, as well as time, specific location and initial pH value were collected as the main independent variables. Due to the fluctuation of environmental variables in the field data and laboratory simulation, the fluctuations measured during the experiment are the maximum and minimum values selected in this study, and the average values given in previous studies.

Also, the concrete corrosion rate was collected to assess the degree of damage to concrete by MICC. The prediction of surface pH can help to judge the stage of corrosion and thus help predict the corrosion rate. Combined with relevant laboratory and field data, 617 samples related to sewer concrete corrosion rate data points were extracted and shown in Tables A.2 (Jiang et al. 2015; Jiang, Keller, and Bond 2014; Lu 2019; Wells and Melchers 2014). The RH and temperature of the field data were also relatively stable, while the H_2S concentration fluctuated greatly. The input variables were the same as those for predicting surface pH except that the two corrosion stages were added.

Different surface pH in stage III and the above-mentioned environmental variables were collected to explore the microbial community succession caused by the interaction between concrete and microbial communities (Jiang et al. 2016; Li et al. 2020, 2021, 2022). Attempt to correlate the influence of environmental factors on corrosion rate with community succession.

2.2. Machine learning model

BPNN updates the entire network by backpropagating the error of the output layer to the weights of the input layer. Both RBFNN and BPNN are feed-forward neural networks with similar structure, consisting of input layer, hidden layer and output layer. Since RBFNN is a local approximation model and BPNN is a global approximation model, the training speed is faster than BPNN, and there is no local minimum problem. BPNN-based ELMNN also a classic feedback neural network based on BPNN. Since the ELMNN neural network adds an inheritance layer to store and utilize the output information of the past time, ELMNN is a dynamic feedback network. The Gaussian process regression (GPR) model is a probabilistic model widely used for predictability. The GPR model includes noise (regression residual) and Gaussian process prior, and the solution method adopts Bayesian inference.

Based on the above information, this study established back propagation neural network (BPNN), radial basis function neural network (RBFNN), Gaussian process regression (GPR), and Elman neural network (ELMNN) to predict the surface pH of concrete and corrosion rate. Input variables include maximum, minimum and average values of H_2S concentration, temperature and RH, as well as time, specific location and initial pH value, stage. In order to prevent the model from overfitting, the data is randomly allocated and the test set and training set are divided according to the ratio of 7:3. And ensure that the size of the data set is within the applicable range of the model, and at the same time add regularization to the model to avoid the occurrence of model overfitting as much as possible. In order to make the model have better prediction accuracy, this study first consulted a large number of literatures to determine

the adjustment range of parameters, and then verified through multiple experiments that keeping its parameters can determine that the model has good prediction ability.

2.3. Model validation

In order to comprehensively evaluate the predictive ability of the model, different indicators are used in this study to evaluate the predictive performance of the model. Theil inequality coefficient (TIC), modified index of agreement (MIA), and Root Mean Square Error (RMSE), R^2, mean absolute error (MAE) were used to evaluate the difference between experimental data and simulated data. Models with the most accurate predictions and superior performance for the predicted values from the collected data typically have TIC values below 0.3, MIA values between [0,1] (Yousuf, Al-Bahadly, and Avci 2021), and have the smallest MSE, RMSE, MAE values, and R^2 value closest to one.

$$RMSE = \sqrt[2]{\frac{1}{N}\sum_{i=1}^{N}\left(y_p - y_o\right)^2} \tag{1}$$

$$MAE = \frac{1}{N}\sum_{i=1}^{N}\left|y_p - y_o\right| \tag{2}$$

$$TIC = \frac{\sqrt{\frac{1}{N}\sum_i\left(y_p - y_o\right)^2}}{\sqrt{\frac{1}{N}\sum_{i=1}^{N} y_p} + \sqrt{\frac{1}{N}\sum_{i=1}^{N} y_o}} \tag{3}$$

$$MIA = 1 - \frac{\sum_i\left|y_{o-y_p}\right|}{\sum_i\left|\overline{y_o} - y_p\right| + \sum_i\left|\overline{y_o} - y_o\right|} \tag{4}$$

$$R^2 = \left[\frac{\frac{1}{N}\sum_{i=1}^{N}\left(y_o - \overline{y_o}\right)\left(y_p - \overline{y_p}\right)}{\sqrt{\frac{1}{N}\sum_{i=1}^{N}\left(y_o - \overline{y_o}\right)^2}\sqrt{\frac{1}{N}\sum_{i=1}^{N}\left(y_p - \overline{y_p}\right)^2}}\right]^2 \tag{5}$$

where N is the number of all experimental data, and y_o and y_p are the experimental data value and predicted value, respectively.

2.4. Correlation analysis

The role of analysis cannot be ignored, and the specific variables collected are not independent of each other. To decipher the correlation coefficients between environmental variables and their potential impact on pipeline corrosion. The yellow solid line indicates that the correlation coefficient between the input variables is positive, the gray dotted line is the opposite, and the thickness of the line represents the strength of the correlation.

3. Results and discussion

3.1. Statistical analysis of concrete corrosion

The average value of environmental factors that demonstrate the effect on surface pH is shown in Fig. A.1. Even a new concrete pipeline with a high concentration of H_2S, i.e. an average concentration between 75 to 750 mg/m^3, would reduce the surface pH of the pipeline to around 4 within a year and reach the MICC of stage III. The average H_2S concentration <10 mg/m^3 was only in stage II of corrosion, even within 4 years. When the concentration of H_2S was lower, the drop of surface pH was greatly delayed.

Figure 1 shows the influence of different concentrations of H_2S on corrosion rates under different stages. The average rate of stage II was about 2 mm/yr, and the highest corrosion rate was about 6 mm/yr. Compared with stage II, the corrosion rate of stage III is significantly higher, with an average corrosion rate of 3 mm/yr and a maximum corrosion rate of 7.5 mm/yr (Figure 1a). When the concentration of H_2S was 15 mg/m^3, except for the average concentration of 750 mg/m^3, the corrosion rates of stage II were higher than other concentrations. The concentration of H_2S was 15 mg/m^3, which may be a critical point. The corrosion rate was maintained at 0-2 mm/yr when the concentration was lower than the critical point. Even if it entered stage III, it maintained a similar corrosion rate. Combined with the surface pH, it could be seen that the H_2S concentration values were less than or equal to 15 mg/m^3, when exposed for 40 months, the surface pH value was stable above 4, while the concentration greater than 15 mg/m^3 caused the surface pH value to drop rapidly and enter stage III. When the concentration of H_2S exceeded the critical point, the corrosion rate of stage II would not increase significantly, and the average values would be below 3 mm/yr, but the corrosion rate of stage III would be greatly accelerated.

The temp.$_{Min}$ was from 17°C-30°C, and the corrosion rates of stage III were about 0.5-1 mm/yr higher than stage II (Figure 2a). Furthermore, it was found that in addition to the temp.$_{Min}$ of 20°C in stage III of corrosion, an increase of temp.$_{Min}$ during the test period increased the corrosion rate. The results of the study indicated that the increase in temperature enhanced the corrosion process (Joseph et al. 2012; Madraszewski et al. 2022). The temp.$_{Max}$ could intuitively reflect that it positively correlates with the corrosion rate. When it reached 37°C, the average corrosion rate was 4 mm/yr. However, the influence of RH on the corrosion rate in the second and third stages of corrosion could not be instantly observed. However, it could be observed that when the RH is 95%, the corrosion rate of stage III was much higher than that of stage II, but this phenomenon was not watched in other RH values. Corrosion rates in stage III were 1 mm/yr higher than stage II in the crown and tidal regions (Fig. A2).

3.2. Prediction of sewer concrete corrosion

3.2.1. Predictive analysis of surface pH

A previous study demonstrated the superiority of artificial neural networks for concrete corrosion and demonstrated that training could significantly improve prediction performance (Jiang et al. 2016; Li et al. 2019; Zounemat-Kermani et al. 2020). Therefore, BPNN, RBFNN, ELMNN, and GPR models for predicting surface pH and corrosion rate are established in MATLAB. To more accurately evaluate the performance of the four models (BPNN, ELMNN, RBFNN, GPR) in predicting sewer concrete, the parameters predicted by different models in the validation set were

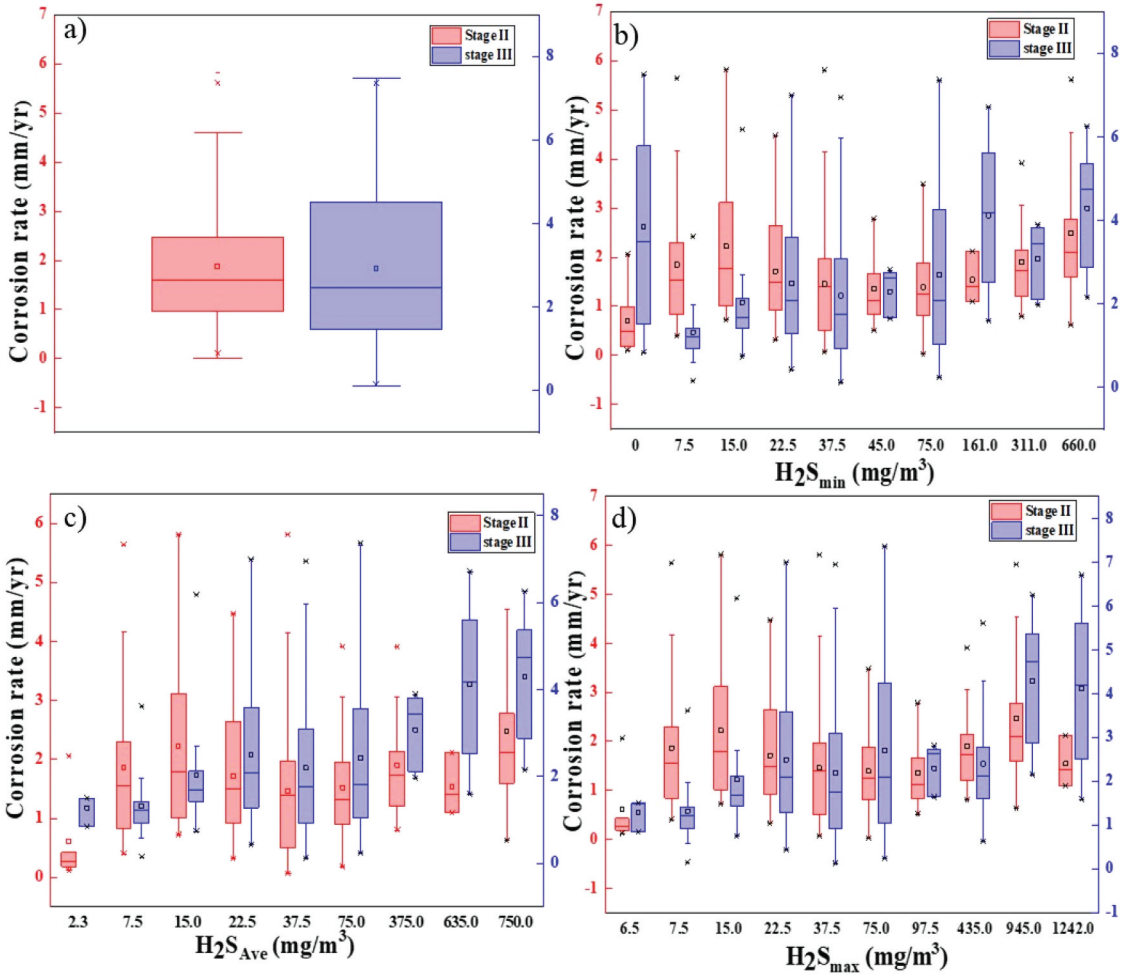

Figure 1. Boxplots of concentrations of H_2S for stage II and stage III versus corrosion rates.

investigated. Table 1 shows the performance of different artificial intelligence models to predict corrosion surface pH and corrosion rate.

To visualize the predictive performance of the model in terms of sewer concrete corrosion, Figure 3(a-d) show the experimental and predicted surface pH. It may be due to too much surface pH data, and it was observed that the extreme learning neural network ELMNN had the disadvantages of slow training speed and easy to fall into local minimum points, and it was difficult to achieve the global optimum after training. Compared with ELMNN, BPNN was more sensitive to the prediction of high corrosion rates. Compared with the prediction results of ANN and ELMNN, GPR and RBFNN had better performance in global prediction. For relatively low corrosion rates, the prediction accuracy of GPR was significantly higher than that of the other three models.

According to Table 1, although BPNN and ELMNN had similar R^2 on the test set, the prediction accuracy of ELMNN was higher than that of BPNN in terms of training set and global prediction. It was observed from the test set R^2 that GPR model had the highest prediction accuracy among the four models, but at the same time, the GPR model was also the model with the worst generalization. Therefore, the model required a large amount of data to be domesticated so that it had good prediction ability. From the prediction parameters of each test set, RBFNN had the highest accuracy rate. This paper recommended using the RBFNN model to predict the surface pH value, so as to judge the current corrosion state of the pipeline.

3.2.2. *Predictive analysis of corrosion rate*

Figure 4 shows a visualization of the predictive performance of the four models on the corrosion rate of sewer concrete. The four models have good performance in predicting the corrosion rate, and it takes work to judge the model's performance through visualization directly. Moreover, In addition, when the corrosion rate is low, the predicted values of the BPNN and RBFNN models appear negative compared with the GPR and ELMNN models.

Unlike the performance of the models predicting the pH of the corrosion surface, all four models showed good predictive performance on the training set. This showed that the selected environmental parameters as characteristic variables could

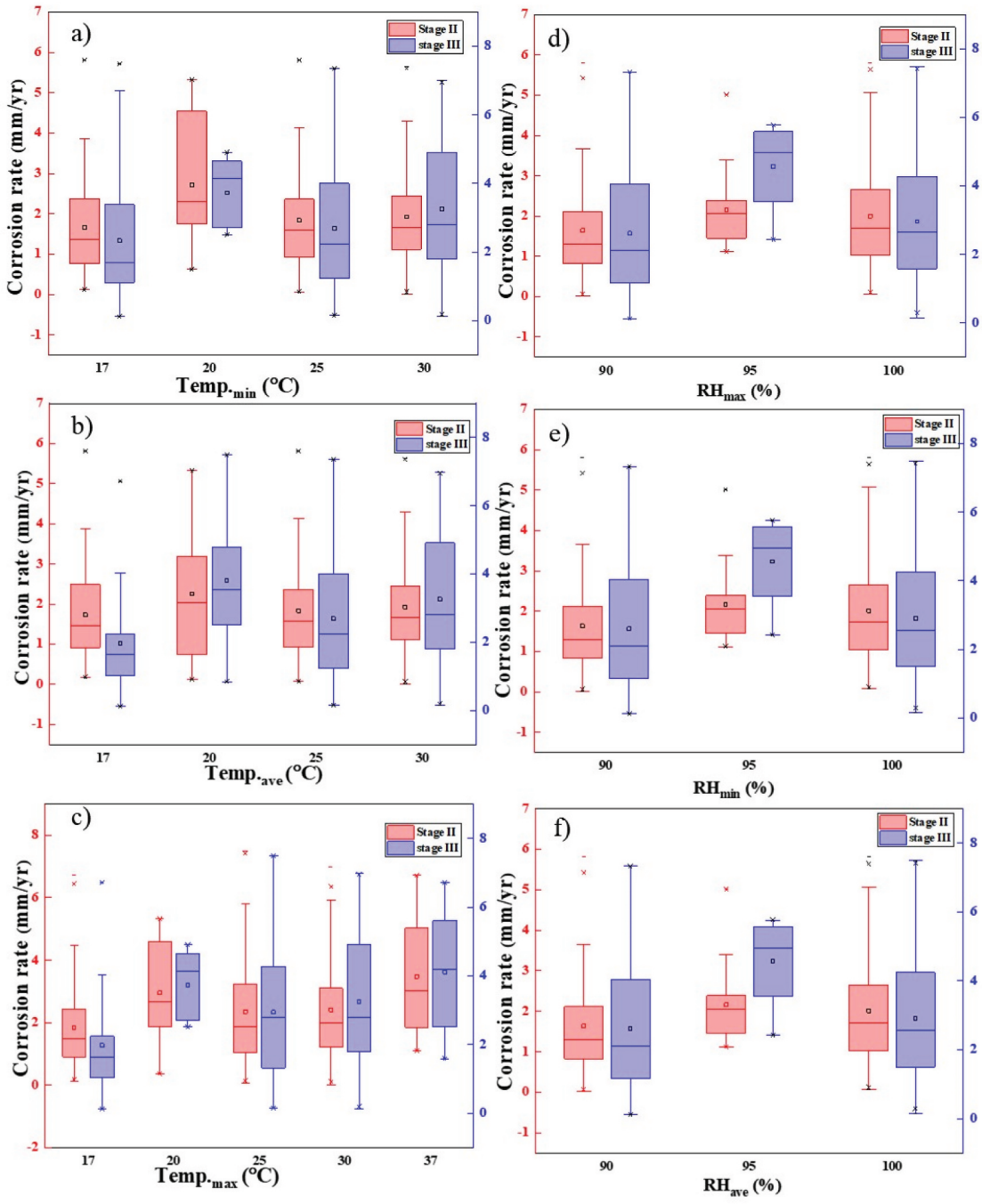

Figure 2. Boxplots of temperature, RH for stage II and stage III versus corrosion rates.

Table 1. Machine learning indicators for predicting concrete.

	Model	R^2_train	R^2_test	RMSE	MSE	MAE	TIC	MIA
Surface pH	BPNN	0.914	0.893	1.12	1.26	0.82	0.07	0.87
	RBFNN	0.912	0.938	0.86	0.74	0.65	0.06	0.90
	ELMNN	0.890	0.912	0.98	0.96	0.73	0.07	0.828
	GPR	0.994	0.832	1.38	1.906	1.09	0.10	0.81
Corrosion rate	BPNN	0.998	0.995	0.32	0.01	0.09	0.01	0.98
	RBFNN	0.999	0.927	0.08	0.70	0.53	0.10	0.90
	ELMNN	0.977	0.968	0.46	0.21	0.35	0.05	0.94
	GPR	0.998	0.823	1.39	1.77	1.08	0.17	0.79

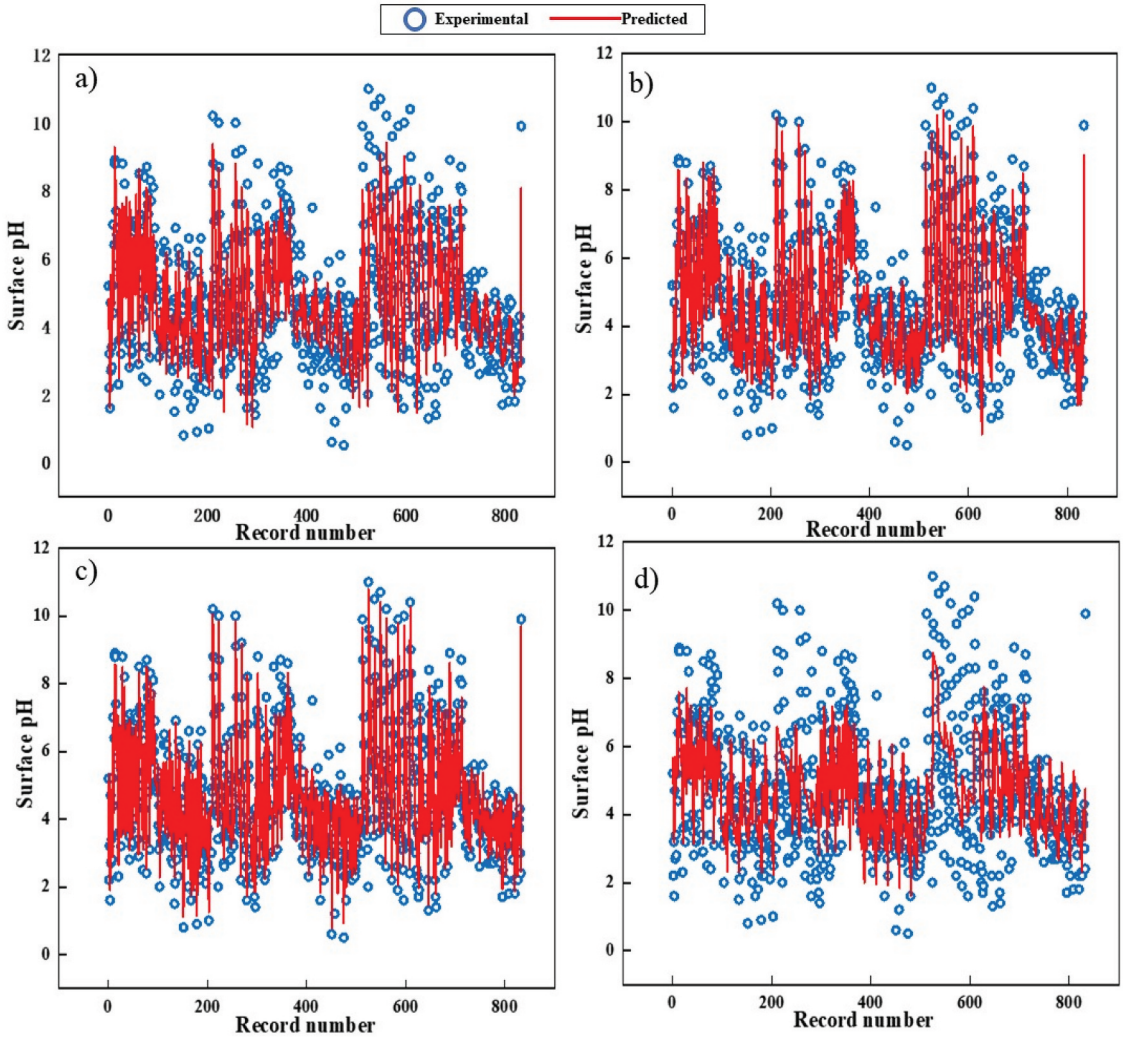

Figure 3. Comparison of the predicted and experimental surface pH by BPNN (a), RBFNN (b), ELMNN (c) and GPR model (d) in the corrosion initiation time data set with the experimental data.

better predict and analyze the process of MICC. Among them, the RBFNN model had the best prediction performance in the test set, $R^2 = 0.999$, but the generalization performance was slightly lacking. From the perspective of generalization performance, BPNN had the best performance, R2 = 0.995, RMSE = 0.32, MSE = 0.01, MAE = 0.09.TIC = 0.01, MIA = 0.98. To prevent the model from overfitting, this study added regularization. Similar to predicting surface pH, GPR model had good predictive performance on the training set, but its predictive ability on the test set was relatively limited, so a large number of training sets could help improve the predictive performance of the GPR model. Therefore, this article recommended using the above characteristic variables as environmental parameters for analysis, and using the BPNN model for prediction.

3.3. Correlation analysis of corrosion parameters

The correlation analysis of stage II and stage III of sewer concrete surface pH and corrosion rate is shown in Figure 5. Explored the mechanism of pipeline deterioration from spearman correlation analysis. The Spearman correlation analysis was used to explore the mechanism analysis of environmental factors on MICC. $Temp._{Max}$ was significantly negatively correlated with pH at stage II, followed by the concrete location and RH_{Min} and H_2S_{Min} concentration. On the contrary, the initial pH positively correlated with the pH, thus delaying the drop in pH. At stage II, the location had the strongest positive correlation with the corrosion rate (Mori et al. 1991, 1992), followed by H_2S concentration and RH (Li et al. 2017). Compared with the drop in surface pH, the influence of temperature on the corrosion rate was relatively limited, but it caused the surface pH to drop rapidly, thus reaching stage III of accelerated corrosion rate. Therefore, the important contributors to stage II of concrete deterioration were the initial pH, temperature, concrete location, and H_2S concentration. At stage III, the environmental variable that had the most lavish impact on the surface pH and corrosion rate was the H_2S concentration, and the deterioration rate of the pipeline will gradually slow down as time goes on (Wells and Melchers 0000, 2016).

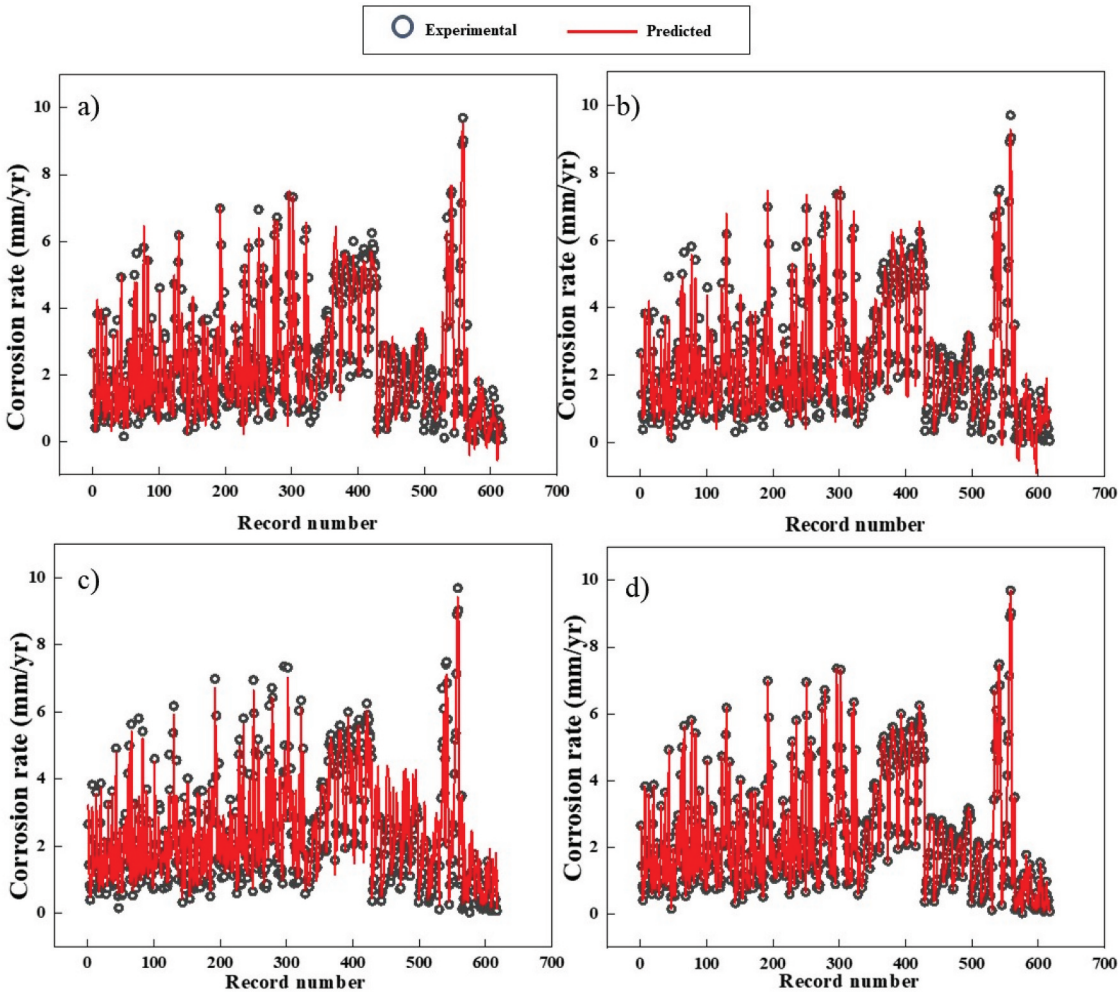

Figure 4. Comparison of the predicted values of the BPNN (a), RBFNN (b), ELMNN (c) and GPR model (d) in the corrosion rate data set with the experimental data.

3.4. Correlation between factors and microbial community

In this study, representative data of different microbial communities on the surface of the corrosion layer in the laboratory and the field were collected from 4 articles, and the effects of three environmental factors (H_2S concentration, RH, temperature) on the relative abundance of the microbial community were analyzed using the RDA method, as shown in Figure 6. Microbial data from stage III were collected due to scarcity of microbial colonization data from stage II. The most common genera such as *Acidophilus*, *Acidithiobacillus*, *Mycobacterium* on corroded concrete surfaces were collected.

The $temp._{Min}$ ranges from 13 to 24, and the RH_{Min} ranges from 82% to 100%. *Acidphilim, Leptospirillum, Acidithiobacillus, Mycobacteria, Microbacterium, Ferroplasma*, and *Acidithiobacillus* were all microbial genera that were greatly affected by $temp._{Min}$ and RH_{Min}. The $temp._{Min}$ and RH_{Min} increase were conducive to the proliferation of *Acidphilim*, *Leptospirillum*, *Acidithiobacillus*, and *Mycobacteria* while inhibiting the growth of *Microbacterium*, *Ferroplasma*. *Acidithiobacillus* was found at a RH_{Min} of 82% to 100% and $temp._{Min}$ of 13°C to 24°C. According to the analysis, RH_{Min} and $temp._{Min}$ increase provided an environment for the growth of *Acidithiobacillus*. When the RH_{Min} rose from 96% to 100%, and $temp._{Min}$ rose from 21 to 24, the relative abundance of *Acidithiobacillus* increased significantly from 25.3 to 99.31. *Leptospirillum* was only found when the RH_{Min} was 100 and the $temp._{Min}$ was 24°C. *Ferroplasma* appeared at a RH_{Min} of 96%-96.4% and $temp._{Min}$ of 21°C. *Microbacterium* accounted for the highest relative abundance when the $temp._{Min}$ was 13 and RH_{Min} was 82%, reaching 35.3%.

The concentration of H_2S ranged from 0 to 1951 mg/m^3. It was observed that H_2S fluctuations had a limited effect on stage IIII of microbial colonization. The enlargement of H_2S concentration was beneficial to reproducing *Microbacterium*, and *Acidithiobacillus*, while inhibiting *Sulfobacillus*, *Mycobacteria*, and *Acidphilim*. *Microbacterium* was found in the average concentration of 12–1239 mg/m^3, accounting for 21%-35% of the relative abundance, and it was observed that the H_2S concentration had a limited effect on the colonization of *Microbacterium*. *Acidithiobacillus* was found to be dominant in the microbial community at H_2S concentrations of 12–37.5 mg/m^3 and sparse at low and high concentrations.

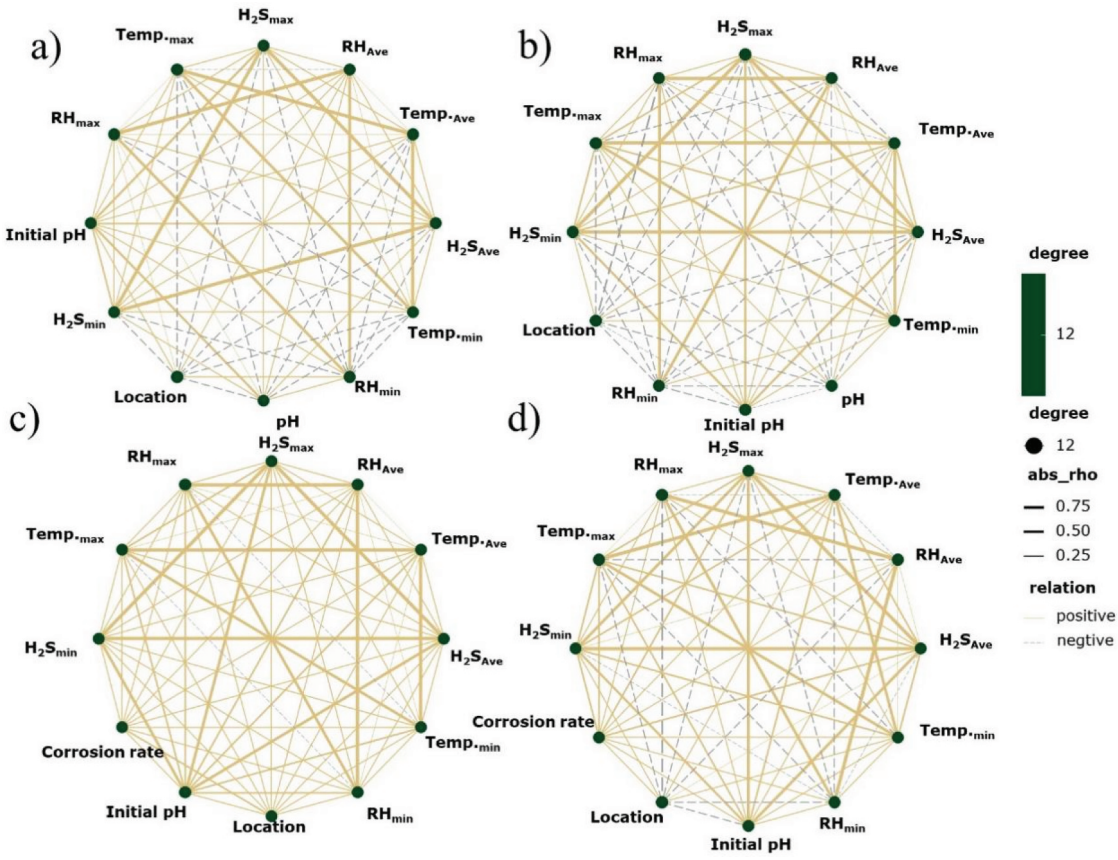

Figure 5. Correlation network of the influence of environmental factors on (a) surface pH at stage II(b) surface pH at stage III (c) corrosion rate at stage II (d) corrosion rate at stage III.

Fluctuations in temperature and RH affected microbial colonization compared to $temp._{Min}$ and RH_{Min}. The increase of the $temp._{max}$ inhibited the growth of *Ralstonia*, *Ferroplasma*, but promoted the reproduction of *Acidphilim*, *Leptospirillum*, *Acidithiobacillus*, *Alicyclobacillus*. The RH_{Max} increase provided conditions for *Alicyclobacillus* to thrive, while *Ralstonia* did the opposite. When the $temp._{max}$ and RH_{Max} were 21°C and 100%, respectively, the proportion of *Ralstonia* reached up to 49.1%.

Acidphilim, *Leptospirillum*, *Acidithiobacillus*, *Ferroplasma* were microbial genera mainly affected by surface pH. *Acidithiobacillus* has been widely found at surface pH 1.6–4. Previous studies also found that when the surface pH < 1, the proportion of *Acidithiobacillus* lowered continuously when the surface pH declined (Pagaling, Yang, and Yan 2014; Song et al. 2019). *Acidphilim* was found in the surface pH range of 3–4, and was found in 3–10 in previous studies (Wu et al. 2020). *Ferroplasma*, relative abundance on the concrete surface, increased significantly when pH < 2 and dominated when the surface pH < 1.35. Leptospirillum was widely found on pipe surfaces when the surface pH is > 1.6.

3.5. Mechanism of concrete corrosion

The presence of H_2S, oxygen and water in the sewer air provides nutrients for microbial corrosion, resulting in microbial corrosion of concrete on the tidal and crown of the sewer pipes, as shown in Figure 7. The average H_2S concentration <15 mg/m^3, which is only in stage II of corrosion, even within 4 years. When the concentration of H_2S exceeded the critical point, the corrosion rate of stage

II would not increase significantly, and the average values would be below 3 mm/yr, but the corrosion rate of stage III would be greatly accelerated. Furthermore, H_2S concentration >75 mg/m^3 will reach stage III of corrosion within one year. In stage III, the environmental variable that has the most lavish impact on the surface pH and corrosion rate is the H_2 S concentration, and the deterioration rate of the pipeline would gradually slow down as time goes on.

The effected of environmental variables and surface pH on microbial community succession were analyzed. When the RH_{Min} rose from 96% to 100%, and the temperature increased from 21°C to 24°C, the relative abundance of acid *Acidithiobacillus* grew significantly from 25.3 to 99.31. Also, when the surface pH < 1, the proportion of *Acidithiobacillus* lowered continuously when the surface pH declined. The environment and surface pH have similar effects on *Microbacterium*, and *Thiobacillus*, all of which adapt to high concentrations of H_2 S and grow as the surface pH drops. And observed that the colonization growth conditions of *Acidphilim*, *Leptospirillum*, *Acidithiobacillus* are similar.

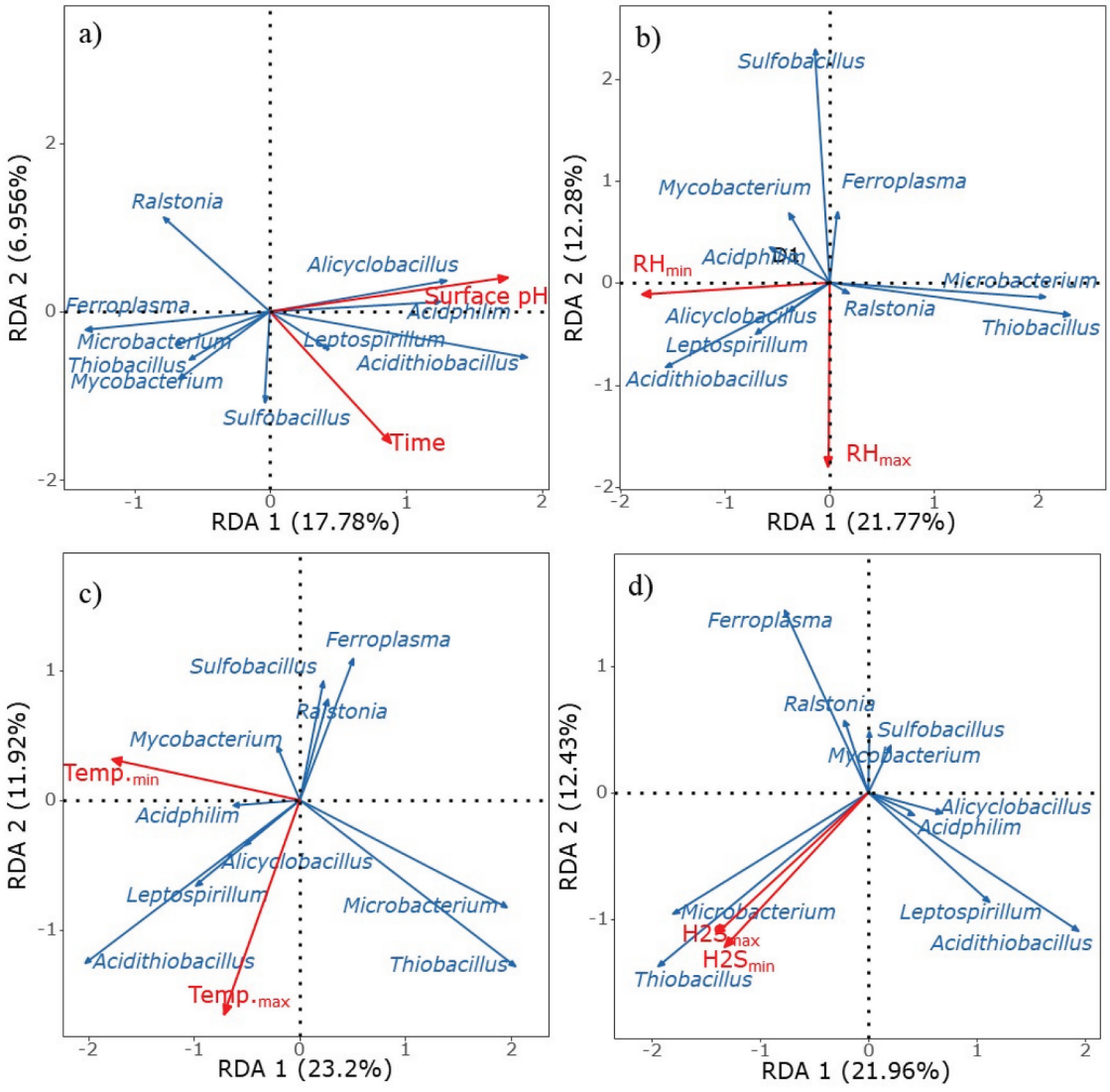

Figure 6. Correlation of microbial genera with (a) surface pH (b) RH(c) temp. And (d) H_2S at stage III.

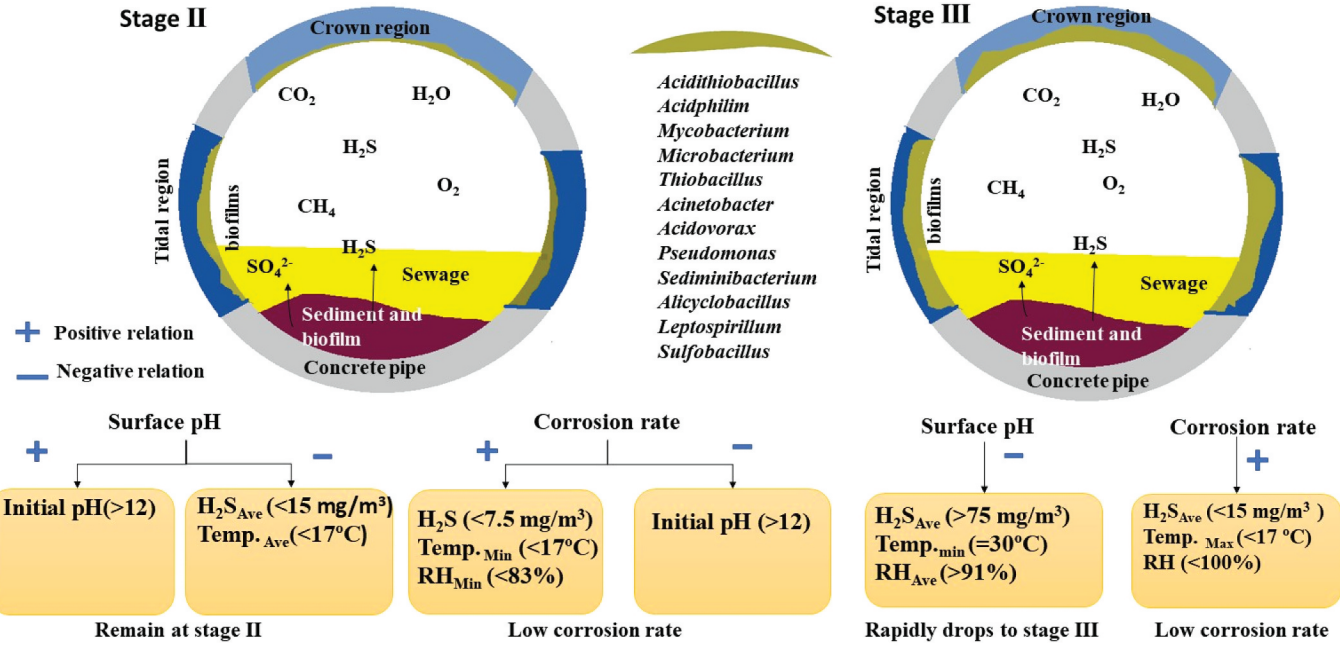

Figure 7. Schematic diagram of corrosion process of sewage pipeline concrete.

4. Conclusions

This study used data, machine learning, and microbial analysis to decipher the impact of environmental factors and surface pH on corrosion rates in stages II and III. The corrosion rate of stage II depended on the concrete's location, and the concrete's corrosion rate in the tidal region is much higher than that in the crown region. In stage II, the concentration of H_2S has a greater effect on the aggravation of corrosion. The corrosion rate of stage II depended on the concrete's location, and the concrete's corrosion rate in the tidal region was much higher than that in the crown region. At stage II, the concentration of H_2S had a greater effect on the aggravation of corrosion. Due to the scarcity of microbial data on colonization at stage II, this paper collected the microbial data of concrete in stage III for analysis. Although previous models can predict laboratory data well, they are only sometimes accurate enough for field corrosion prediction. The input variables are minimum, maximum and average H_2S concentration, RH, temperature, initial pH, MICC stage and specific location to better predict and analyze corrosion rate (R^2 >0.999).

Although concrete composition plays an important role in the resistance to MICC, the relevant description is limited due to most of the experimental concrete samples tested. More concrete components use chemical methods to evaluate the corrosion resistance in the study of MICC resistance, so the next step of research should focus on exploring the impact of concrete-related parameters on MICC. And with the development of research in recent years, the detection of pipe surface temperature and relative humidity may be more helpful for the analysis of pipe wall corrosion (Thiyagarajan et al. 2018, 2020). The underground subsurface pH condition is a crucial evaluation index for monitoring sewer corrosion, so the detection of underground subsurface pH is equally important.

Acknowledgements

This research did not receive any specific grant from funding agencies in the public, commercial, or not-for-profit sectors.

Disclosure statement

No potential conflict of interest was reported by the author(s).

Data availability statement

All data presented herein will be provided upon reasonable request.

Author's contribution statement

Wenhao Wang: Investigation, Methodology, Writing. Xinxin xu: Concepts, Methodology, Writing – review & editing; Jingguo Cao: Supervision, Project administration; Ming Zeng: Supervision, Methodology; Wu Zhang, Investigation.

References

Abuhishmeh, K. S. 2019. "Service life prediction and risk analysis of reinforced concrete gravity flow pipes using reliability theory". Master's thesis, The University of Texas at Arlington.

Abuhishmeh, K., and H. H. Jalali. 2023. "Reliability Assessment of Reinforced Concrete Sewer Pipes Under Adverse Environmental Conditions: Case Study for the City of Arlington, Texas." *Journal of Pipeline Systems Engineering and Practice* 14 (2): 05023001. https://doi.org/10.1061/JPSEA2.PSENG-1406.

Allahverdi, A., and F. J. C. S. Škvára. 2000. "Acidic Corrosion of Hydrated Cement Based Materials", *Ceram. Silikáty* 44 (4): 152–160.

Bielefeldt, A., M. G. D. Gutierrez-Padilla, S. Ovtchinnikov, J. Silverstein, and M. Hernandez. 2010. "Bacterial Kinetics of Sulfur Oxidizing Bacteria and Their Biodeterioration Rates of Concrete Sewer Pipe Samples." *Journal of Environmental Engineering* 136 (7): 731–738. https://doi.org/10.1061/(ASCE)EE.1943-7870.0000215.

Cayford, B. I., P. G. Dennis, J. Keller, G. W. Tyson, and P. L. Bond. 2012. "High-Throughput Amplicon Sequencing Reveals Distinct Communities within a Corroding Concrete Sewer System." *Applied and Environmental Microbiology* 78 (19): 7160–7162. https://doi.org/10.1128/AEM.01582-12.

Deng, Y., X. Zhou, J. Shen, G. Xiao, H. Hong, H. Lin, F. Wu, and B. Q. Liao. 2021. "New Methods Based on Back Propagation (Bp) and Radial Basis Function (Rbf) Artificial Neural Networks (Anns) for Predicting the Occurrence of Haloketones in Tap Water." *The Science of the Total Environment* 772:145534. https://doi.org/10.1016/j.scitotenv.2021.145534.

Ebrahimi, M., H. Hojat Jalali, and S. Sabatino. 2023. "Probabilistic Condition Assessment of Reinforced Concrete Sanitary Sewer Pipelines Using Lidar Inspection Data." *Automation in Construction* 150:104857. https://doi.org/10.1016/j.autcon.2023.104857.

Ebrahimi, M., and H. H. Jalali, 2022a. *Automated Condition Assessment of Sanitary Sewer Pipes Using Lidar Inspection Data %j Pipelines 2022*.

Ebrahimi, M., and H. H. Jalali, 2022b. *Spatial Variability Effects of Wall Erosion on Assessment of Reinforced Concrete Sanitary Sewer Pipes (Rcssps) %j Tran-Set 2022*.

Grengg, C., F. Mittermayr, G. Koraimann, F. Konrad, M. Szabó, A. Demeny, and M. Dietzel. 2017. "The Decisive Role of Acidophilic Bacteria in Concrete Sewer Networks: A New Model for Fast Progressing Microbial Concrete Corrosion." *Cement and Concrete Research* 101:93–101. https://doi.org/10.1016/j.cemconres.2017.08.020.

Grengg, C., F. Mittermayr, N. Ukrainczyk, G. Koraimann, S. Kienesberger, and M. Dietzel. 2018. "Advances in Concrete Materials for Sewer Systems Affected by Microbial Induced Concrete Corrosion: A Review." *Water Research* 134:341–352. https://doi.org/10.1016/j.watres.2018.01.043.

Gutberlet, T., H. Hilbig, and R. E. Beddoe. 2015. "Acid Attack on Hydrated Cement — Effect of Mineral Acids on the Degradation Process." *Cement and Concrete Research* 74:35–43. https://doi.org/10.1016/j.cemconres.2015.03.011.

Ismail, N., T. Nonaka, S. Noda, and T. J. D. G. R. Mori. 1993. "Effect of Carbonation on Microbial Corrosion of Concretes." *Doboku Gakkai Ronbunshu* 1993 (474): 133–138.

Jiang, G., J. Keller, and P. L. Bond. 2014. "Determining the Long-Term Effects of H(2)s Concentration, Relative Humidity and Air Temperature on Concrete Sewer Corrosion." *Water Research* 65:157–169. https://doi.org/10.1016/j.watres.2014.07.026.

Jiang, G., J. Keller, P. L. Bond, and Z. Yuan. 2016. "Predicting Concrete Corrosion of Sewers Using Artificial Neural Network." *Water Research* 92:52–60. https://doi.org/10.1016/j.watres.2016.01.029.

Jiang, G., Y. Liu, X. Li, and X. Sun. 2023. *Mathematical Modelling for the Concrete Corrosion of Sewer Systems*. Microbiologically Influenced Corrosion of Concrete Sewers: Mechanisms, Measurements, Modelling and Control Strategies, pp. 159–181. Springer International Publishing. https://doi.org/10.1007/978-3-031-29941-4_8.

Jiang, G., X. Sun, J. Keller, and P. L. Bond. 2015. "Identification of Controlling Factors for the Initiation of Corrosion of Fresh Concrete Sewers." *Water Research* 80:30–40. https://doi.org/10.1016/j.watres.2015.04.015.

Jiang, G., X. Sun, J. Keller, and P. L. J. W. R. Bond. 2015. "Identification of Controlling Factors for the Initiation of Corrosion of Fresh Concrete

Sewers." *Water Research* 80:30–40. https://doi.org/10.1016/j.watres.2015.04.015.

Jiang, G., M. Zhou, T. H. Chiu, X. Sun, J. Keller, and P. L. Bond. 2016. "Wastewater-Enhanced Microbial Corrosion of Concrete Sewers." *Environmental Science and Technology* 50 (15): 8084–8092. Available from. https://www.ncbi.nlm.nih.gov/pubmed/27390870.

Joseph, A. P., J. Keller, H. Bustamante, and P. L. Bond. 2012. "Surface Neutralization and H(2)s Oxidation at Early Stages of Sewer Corrosion: Influence of Temperature, Relative Humidity and H(2)s Concentration." *Water Research* 46 (13): 4235–4245. Available from. https://www.ncbi.nlm.nih.gov/pubmed/22677502.

Li, X. 2020. "Understanding and Controlling of Concrete Corrosion in Sewers." PhD Thesis, School of Chemical Engineering, The University of Queensland.

Li, X., P. L. Bond, L. O'moore, S. Wilkie, L. Hanzic, I. Johnson, K. Mueller, Z. Yuan, and G. Jiang. 2020. "Increased Resistance of Nitrite-Admixed Concrete to Microbially Induced Corrosion in Real Sewers." *Environmental Science and Technology* 54 (4): 2323–2333. Available from. https://www.ncbi.nlm.nih.gov/pubmed/31977201.

Li, X., I. Johnson, K. Mueller, S. Wilkie, L. Hanzic, P. L. Bond, L. O'moore, Z. Yuan, and G. Jiang. 2022. "Corrosion Mitigation by Nitrite Spray on Corroded Concrete in a Real Sewer System." *The Science of the Total Environment* 806 (Pt 3): 151328. Available from. https://www.ncbi.nlm.nih.gov/pubmed/34743876.

Li, X., U. Kappler, G. Jiang, and P. L. Bond. 2017. "The Ecology of Acidophilic Microorganisms in the Corroding Concrete Sewer Environment." *Frontiers in Microbiology* 8:683. https://doi.org/10.3389/fmicb.2017.00683.

Li, X., F. Khademi, Y. Liu, M. Akbari, C. Wang, P. L. Bond, J. Keller, and G. Jiang. 2019. "Evaluation of Data-Driven Models for Predicting the Service Life of Concrete Sewer Pipes Subjected to Corrosion." *Journal of Environmental Management* 234:431–439. https://doi.org/10.1016/j.jenvman.2018.12.098.

Li, X., J. Kulandaivelu, L. O'moore, S. Wilkie, L. Hanzic, P. L. Bond, Z. Yuan, and G. Jiang. 2021. "Synergistic Effect on Concrete Corrosion Control in Sewer Environment Achieved by Applying Surface Washing on Calcium Nitrite Admixed Concrete." *Construction and Building Materials* 302:124184. https://doi.org/10.1016/j.conbuildmat.2021.124184.

Li, X., L. O'moore, Y. Song, P. L. Bond, Z. Yuan, S. Wilkie, L. Hanzic, and G. Jiang. 2019. "The Rapid Chemically Induced Corrosion of Concrete Sewers at High h2s Concentration." *Water Research* 162:95–104. https://doi.org/10.1016/j.watres.2019.06.062.

Liu, Y., Y. Song, J. Keller, P. Bond, and G. Jiang. 2017. "Prediction of Concrete Corrosion in Sewers with Hybrid Gaussian Processes Regression Model." *RSC Advances* 7 (49): 30894–30903. https://doi.org/10.1039/C7RA03959J.

Lu, H., 2019. *Accelerated simulation study on the corrosion of non-full flow concrete sewers (master's thesis)*. master.

Madraszewski, S., F. Dehn, J. Gerlach, and D. Stephan. 2022. "Experimentally Driven Evaluation Methods of Concrete Sewers Biodeterioration on Laboratory-Scale: A Critical Review." *Construction and Building Materials* 320:126236. https://doi.org/10.1016/j.conbuildmat.2021.126236.

Mori, T., M. Koga, Y. Hikosaka, T. Nonaka, F. Mishina, Y. Sakai, J. J. W. S. Koizumi, and Technology. 1991. "Microbial Corrosion of Concrete Sewer Pipes, h2s Production from Sediments and Determination of Corrosion Rate." *Water Science & Technology* 23 (7–9): 1275–1282. https://doi.org/10.2166/wst.1991.0579.

Mori, T., T. Nonaka, K. Tazaki, M. Koga, Y. Hikosaka, and S. J. W. R. Noda. 1992. "Interactions of Nutrients, Moisture and Ph on Microbial Corrosion of Concrete Sewer Pipes." *Water Research* 26 (1): 29–37. https://doi.org/10.1016/0043-1354(92)90107-F.

O'connell, M., C. Mcnally, and M. G. Richardson. 2010. "Biochemical Attack on Concrete in Wastewater Applications: A State of the Art Review." *Cement and Concrete Composites* 32 (7): 479–485. https://doi.org/10.1016/j.cemconcomp.2010.05.001.

Okabe, S., M. Odagiri, T. Ito, and H. Satoh. 2007. "Succession of Sulfur-Oxidizing Bacteria in the Microbial Community on Corroding Concrete in Sewer Systems." *Applied & Environmental Microbiology* 73 (3): 971–980. Available from. https://www.ncbi.nlm.nih.gov/pubmed/17142362.

Pagaling, E., K. Yang, and T. Yan. 2014. "Pyrosequencing Reveals Correlations Between Extremely Acidophilic Bacterial Communities with Hydrogen Sulphide Concentrations, Ph and Inert Polymer Coatings at Concrete Sewer Crown Surfaces." *Journal of Applied Microbiology* 117 (1): 50–64. Available from. https://www.ncbi.nlm.nih.gov/pubmed/24606006.

Satoh, H., M. Odagiri, T. Ito, and S. Okabe. 2009. "Microbial Community Structures and in situ Sulfate-Reducing and Sulfur-Oxidizing Activities in Biofilms Developed on Mortar Specimens in a Corroded Sewer System." *Water Research* 43 (18): 4729–4739. Available from. https://www.ncbi.nlm.nih.gov/pubmed/19709714.

Song, Y., Y. Tian, X. Li, J. Wei, H. Zhang, P. L. Bond, Z. Yuan, and G. Jiang. 2019. "Distinct Microbially Induced Concrete Corrosion at the Tidal Region of Reinforced Concrete Sewers." *Water Research* 150:392–402. https://doi.org/10.1016/j.watres.2018.11.083.

Sun, X., G. Jiang, P. L. Bond, and J. Keller. 2015. "Impact of Fluctuations in Gaseous h2s Concentrations on Sulfide Uptake by Sewer Concrete: The Effect of High h2s Loads." *Water Research* 81:84–91. https://doi.org/10.1016/j.watres.2015.05.044.

Sun, X., G. Jiang, P. L. Bond, and J. Keller. 2019. "Periodic Deprivation of Gaseous Hydrogen Sulfide Affects the Activity of the Concrete Corrosion Layer in Sewers." *Water Research* 157:463–471. https://doi.org/10.1016/j.watres.2019.03.074.

Sun, X., G. Jiang, P. L. Bond, T. Wells, and J. Keller. 2014. "A Rapid, Non-Destructive Methodology to Monitor Activity of Sulfide-Induced Corrosion of Concrete Based on h2s Uptake Rate." *Water Research* 59:229–238. https://doi.org/10.1016/j.watres.2014.04.016.

Thiyagarajan, K., S. Kodagoda, R. Ranasinghe, D. Vitanage, and G. J. I. S. J. Iori. 2020. "Robust Sensor Suite Combined with Predictive Analytics Enabled Anomaly Detection Model for Smart Monitoring of Concrete Sewer Pipe Surface Moisture Conditions." *IEEE Sensors Journal* 20 (15): 8232–8243. https://doi.org/10.1109/JSEN.2020.2982173.

Thiyagarajan, K., S. Kodagoda, R. Ranasinghe, D. Vitanage, and G. J. S. R. Iori. 2018. "Robust Sensing Suite for Measuring Temporal Dynamics of Surface Temperature in Sewers." *Scientific Reports* 8 (1): 16020. https://doi.org/10.1038/s41598-018-34121-3.

Vollertsen, J., A. H. Nielsen, H. S. Jensen, T. Wium-Andersen, and T. Hvitved-Jacobsen. 2008. "Corrosion of Concrete Sewers–The Kinetics of Hydrogen Sulfide Oxidation." *The Science of the Total Environment* 394 (1): 162–170. Available from. https://www.ncbi.nlm.nih.gov/pubmed/18281080.

Wang, Y., P. Li, H. Liu, W. Wang, Y. Guo, and L. Wang. 2022. "The Effect of Microbiologically Induced Concrete Corrosion in Sewer on the Bearing Capacity of Reinforced Concrete Pipes: Full-Scale Experimental Investigation." *Buildings* 12 (11): 1996. https://doi.org/10.3390/buildings12111996.

Wang, Y., P. Li, L. J. J. O. T. Wang, and Evaluation. 2022. "The Testing Methods and Prediction Models for Concrete Corrosion in Sewer Pipelines: A State-Of-The-Art Review." *Journal of Testing and Evaluation* 50 (5): 2791–2815. https://doi.org/10.1520/JTE20210702.

Wang, Y., F. Su, Y. Guo, H. Yang, Z. Ye, and L. Wang. 2022. "Predicting the Microbiologically Induced Concrete Corrosion in Sewer Based on Xgboost Algorithm." *Case Studies in Construction Materials* 17:17. https://doi.org/10.1016/j.cscm.2022.e01649.

Wang, Y., F. Su, P. Li, W. Wang, H. Yang, and L. Wang. 2023. "Microbiologically Induced Concrete Corrosion in the Cracked Sewer Pipe Under Sustained Load." *Construction and Building Materials* 369:130521. https://doi.org/10.1016/j.conbuildmat.2023.130521 .

Wells, T., and R. Melchers. Year. Findings of a 4 Year Study of Concrete Sewer Pipe Corrosion.^eds. *Annual Conference of the Australasian Corrosion Association*Australasian Corrosion Association Preston, Victoria, Australia, 1–12.

Wells, T., and R. E. Melchers. 2014. "An Observation-Based Model for Corrosion of Concrete Sewers Under Aggressive Conditions." *Cement and Concrete Research* 61-62:1–10. https://doi.org/10.1016/j.cemconres.2014.03.013.

Wells, T., and R. J. P. O. T. O. Melchers. 2016. "Concrete Sewer Pipe Corrosion —Findings from an Australia Field Study."

Wu, M., T. Wang, K. Wu, and L. Kan. 2020. "Microbiologically Induced Corrosion of Concrete in Sewer Structures: A Review of the Mechanisms and Phenomena." *Construction and Building Materials* 239:117813. https://doi.org/10.1016/j.conbuildmat.2019.117813.

Yousuf, M. U., I. Al-Bahadly, and E. Avci. 2021. "A Modified Gm(1,1) Model to Accurately Predict Wind Speed." *Sustainable Energy Technologies and Assessments* 43:100905. Available from https://www.sciencedirect.com/science/article/pii/S2213138820313321. https://doi.org/10.1016/j.seta.2020.100905.

Yuan, H., P. Dangla, P. Chatellier, and T. Chaussadent. 2015. "Degradation Modeling of Concrete Submitted to Biogenic Acid Attack." *Cement and Concrete Research* 70:29–38. https://doi.org/10.1016/j.cemconres.2015.01.002.

Zounemat-Kermani, M., D. Stephan, M. Barjenbruch, and R. Hinkelmann. 2020. "Ensemble Data Mining Modeling in Corrosion of Concrete Sewer: A Comparative Study of Network-Based (MLPNN & RBFNN) and Tree-Based (RF, CHAID, & CART) Models." *Advanced Engineering Informatics* 43:101030. https://doi.org/10.1016/j.aei.2019.101030.